Proceedings World Geothermal Congress 2010
Bali, Indonesia, 25-29 April 2010

Reservoir Induced Seismicity: Where, When, Why and How Strong?

Stefan Baisch and Robert Vörös

Q-con GmbH, Markstr. 39, D-76887 Bad Bergzabern, Germany

baisch@q-con.de

Keywords: Enter reservoir stimulation, seismic risk, numerical models

ABSTRACT

With the increasing number of (deep) geothermal projects in industrialized regions, the potential risk associated with reservoir induced seismicity has become a critical point of discussion. A detailed understanding of the physical processes associated with reservoir induced seismicity is required for assessing and (eventually) mitigating the seismic risk.

We present a hydro-mechanical model describing fluid injection induced seismicity. The model is based on the physical processes of fluid pressure and stress diffusion with triggering of the induced seismicity being controlled by Coulomb friction. Earthquake magnitudes are primarily determined by the rupture area, i.e. the spatial extend over which fracture critically is exceeded coseismically.

We use a three-dimensional finite element implementation of the model to simulate in situ hydraulic overpressures and induced seismicity for a typical hydraulic stimulation scenario. The model seismicity exhibits similar features as observed at various geothermal sites. These include the spatio-temporal seismicity distribution with a strong manifestation of the Kaiser Effect, event magnitude distributions, and the occurrence of the largest magnitude events after shut-in of the injection well.

Our results demonstrate that characteristic observations of the induced seismicity can be explained already with a relatively simple physical model with almost no *a priori* assumptions. In particular, the increase of the event magnitudes with stimulation duration can be attributed to a geometrical effect, where stress criticality is approached over a larger reservoir area. The numerical implementation of our hydro-mechanical model provides a powerful tool for addressing the seismic risk associated with reservoir stimulations.

1. INTRODUCTION

Shear dilation stimulation, which implies injection of large fluid volumes at high pressure, has become a standard technology for the development of deep geothermal reservoirs (**E**nhanced **G**eothermal **S**ystems, EGS). Especially in crystalline host rock, these stimulations are accompanied by vast amounts of induced seismicity (e.g. Davis and Frohlich, 1993). Although most of the induced seismicity is of small magnitude only, isolated events of larger magnitude were induced in the past (Baisch et al., 2009b).

The most prominent example is an M=3.4 event induced by the stimulation of a geothermal reservoir below the city of Basel (Switzerland) which led to a (preliminary) termination of the project (Häring et al., 2008). At the geothermal site of Soultz-sous-Forêts (France), stimulation of the deep reservoir produced seismic events with magnitudes of up to M=2.9 (Dorbath et al., 2009) raising major concerns about potential damage. Interestingly, the largest magnitude events seem to occur predominantly in the shut-in period after fluid injection has been terminated (Baisch et al., 2009b). This complicates the application of "traffic light systems" where hydraulic injection is aborted whenever seismicity exceeds a critical magnitude threshold (Bommer et al., 2006). Clearly, a more detailed understanding of the physical processes associated with induced seismicity is required to enable a large scale application of the EGS technology.

In the first section of this paper we discuss characteristic observations of induced seismicity made at the geothermal sites of Basel (Switzerland), Soultz-sous-Forêts (France), and Cooper Basin (Australia). At these sites, the spatial distribution of the induced seismicity predominantly aligns along a larger scale fault (zone). Based on these observations, we developed a numerical model to simulate induced seismicity during hydraulic stimulations in a fault zone. Without invoking any structural complexity, the numerical model successfully reproduces characteristics of the induced seismicity typically observed during fluid injection experiments.

2. CHARACTERISTICS OF INDUCED SEISMICITY

Deep Reservoir at Soultz-sous-Forêts

Seismicity induced during the stimulation of the deeper reservoir at Soultz-sous-Forêts has been analyzed in a large number of studies. Different conclusions were made concerning the reservoir geometry as outlined by the distribution of the induced seismicity. For example, Michelet & Töksöz (2007) find a volumetric distribution rather than the planar structure obtained by Charlety et al. (2007). Baisch et al. (2009b) reprocessed the data set of Michelet & Töksöz (2007) and conclude that the volumetric structure obtained by these authors is an artefact of data scattering. Figure 1 shows the seismicity distribution determined by Baisch et al. (2009b). The seismicity aligns along a subvertical, planar structure with slight curvature. This further confirms the conclusion of Charlety et al. (2007) that the deeper reservoir is dominated by one or several large scale faults.

Larger parts of the fault structure identified in Figure 1 might be oriented favourable for shear in the local stress field where maximum and minimum stresses are horizontal and S_H strikes at N170° (Cornet et. al. 2007). This indicates that the seismic activity at Soultz-sous-Forêts occurs on patches of a larger scale fault.

Figure 2 compares hypocenter locations of the seismic activity induced during the stimulation of the GPK3 well with the locations of the seismic activity occurring after shut-in. Interestingly, the vicinity of the injection well remains seismically quiet in the post-injection period, whereas seismic activity solely occurs at the outer rim of

the zone of previous seismicity. We will demonstrate in a later section that the region of post-injection seismic activity coincides with those locations, where fluid overpressures keep increasing after shut-in.

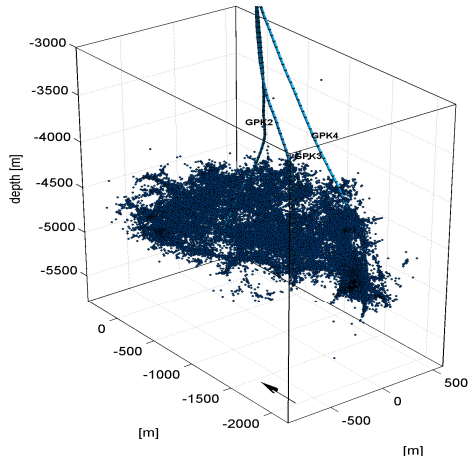

Figure 1: Hypocenter distribution of the induced seismicity at Soultz-sous-Forêts (deeper reservoir) after data collapsing. Solid lines indicate the trajectories of the wells GPK2, GPK3, and GPK4, respectively.

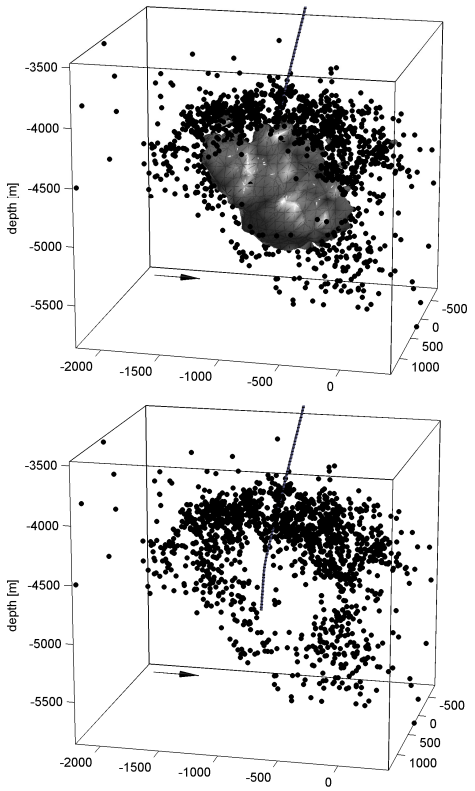

Figure 2: Comparison between the seismic activity induced during the ~10 days stimulation of the GPK-3 well (solid line) and the seismicity occurring during the first 2.5 days of the shut-in period (dots). Seismic activity during stimulation is shown by an iso-surface of the hypocenter density drawn at 3 events per cubic bin of 80 m side length (top). Note that post-injection seismicity occurs exclusively at the outer rim of the previously stimulated zone (bottom). Figure taken from Baisch et al. (2006b).

The seismicity distribution shown in Figure 2 thus can be interpreted as a manifestation of the Kaiser effect (Baisch and Harjes, 2003), with the occurrence of seismicity being restricted to those areas where previously experienced fluid overpressures are exceeded.

Cooper Basin Reservoir

During the stimulation of a geothermal reservoir in the Cooper Basin (Australia) more than 45,000 seismic events were induced with magnitudes up to M=3.7 (Baisch et al., 2006, 2009). Figure 3 shows the hypocenter distribution obtained for the first stimulation period in 2003. Seismic activity aligns along a subhorizontal, planar structure. Baisch et al. (2006) have demonstrated that the actual height of the structure is at (or even below) the meter scale which has been confirmed by subsequent wells drilled into the reservoir.

The stress regime in the Cooper Basin is thrust faulting with S_H being oriented approximately East-West. This indicates that the seismic activity in the Cooper Basin reservoir occurs on patches of a larger scale fault and is driven by the local stress field (Baisch et al., 2009). In this respect, the scenario is amazingly similar to the situation at Soultz-sous-Forêts when accounting for a 90 deg rotation of the local stress field.

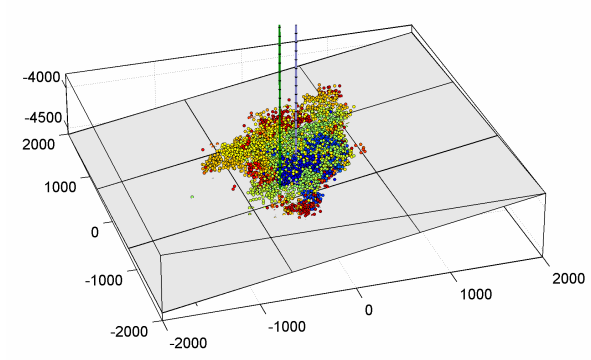

Figure 3: Hypocenter distribution of the induced seismicity in the Cooper Basin (Australia). Hypocenters align along a subhorizontal structure with the thickness being dominated by data scattering.

The seismic activity in the Cooper Basin exhibits a high degree of spatio-temporal order. Early seismicity starts at the injection well (Figure 4) and systematically migrates outwards with increasing duration of the stimulation. Again, this can be explained by the Kaiser Effect, where the near well region experienced its peak hydraulic overpressures already during an early stage of the stimulation and therefore remained seismically quiet at later times.

Basel Reservoir

By stimulation activities of a geothermal reservoir underneath the city of Basel (Switzerland), nearly 15,000 seismic events have been induced (Häring et al., 2008). Associated hypocenters predominantly align along a subvertical, north-west trending structure with limited width (Figure 7 of Häring et al., 2008) similar to the scenario obtained for the Soultz-sous-Forêts reservoir (Figure 1). Consistent with observations at Soultz-sous-Forêts and in the Cooper Basin, post-injection seismicity at Basel solely occurs at the outer rim of the zone of previous seismic activity (Figure 7 of Häring et al., 2008). This

indicates that the Kaiser Effect is a characteristic feature common to all three geothermal reservoirs discussed here.

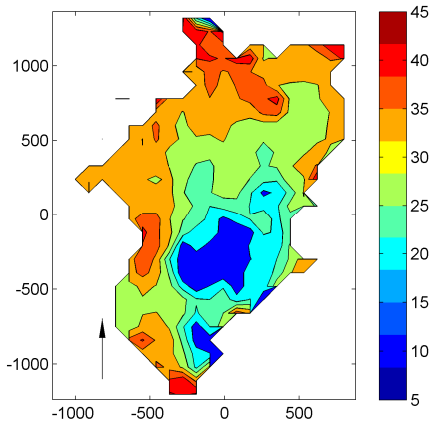

Figure 4: Spatio-temporal distribution of the seismicity induced in the Cooper Basin in map view displayed by contours of the occurrence times according to the colour scaling. Occurrence times are given in days with respect to the start of the injection and are averaged over cubic bins of 50 m side length. Figure after Baisch et al., 2006.

3. HYDRO-MECHANICAL MODEL

In the previous section we have demonstrated that the seismic activity induced at different geothermal sites commonly aligns along approximately two-dimensional structures which most likely reflect pre-existing faults. The existence of large scale structures is also supported by the fact that relatively strong earthquakes have occurred in these reservoirs which typically require shearing planes in the order of several 10,000 m^2. Therefore we have chosen the simplest geometry of a single fault as the basis for our numerical models.

Following previous considerations of potential triggering mechanisms for the induced seismicity at Soultz-sous-Forêts (Baisch et al., 2006b), in the Cooper Basin (Baisch et al., 2006), and at Basel (Häring et al., 2008), we assume that the seismic activity is driven by the Hubbert-Ruby mechanism (Hsieh and Bredehoeft, 1981): Hydraulic overpressures reduce the effective normal stress acting on existing fractures until the ratio between shear- and effective normal stress exceeds the coefficient of friction and shear slippage occurs.

In our hydro-mechanical model we assume that the large-scale fault consists of many smaller fault patches which may slip independently but are mechanically coupled to their neighbours (so called “block-spring model”, e.g. Bak & Tang, 1989). Whenever shear slip occurs, the shear stress resolved on the patch is reduced by the amount of stress drop and shear stress on the neighbouring patches is increased due to mechanical coupling. For details of the stress transfer pattern we refer to Baisch et al. (2009b). Due to stress redistribution, slip on an individual patch may cause overcritical stress conditions on neighbouring patches, thus triggering an “avalanche” of simultaneous slip events. The strength of a seismic shear event can be described by its seismic moment which is proportional to the shearing area, or in other words to the number of patches slipping simultaneously.

4. MODELLED SEISMICITY

We implemented the hydro-mechanical model discussed in the previous section into a numerical finite-element model. Fault parameters (e.g. orientation, resolved stresses, and coefficient of friction) have been adapted from observations made at Soultz-sous-Forêts and the injection history mimics the stimulation of the GPK2 well (see Baisch et al., 2009b for details).

A total number of 24,872 slip events were triggered during the 20 days simulation time. Magnitudes of these events are between M=-1.1 and M=2.8, where the lower magnitude limit reflects the minimum patch size of 20 m side length.

Figure 5 shows the temporal evolution of the event magnitudes. Besides a few scattered events with comparatively large magnitudes (i.e. around M=2) occurring at an early stage of the injection, the maximum event magnitude tends to increase with time during the stimulation. This becomes most evident during shut-in and we notice that the largest magnitude event occurred approximately 6.5 days after shut-in. Figure 6 shows the spatial distribution of hydraulic overpressures at the time when the largest magnitude event occurred. The location of this event is at the outer rim of the zone of previous seismic activity. Here, fluid overpressures keep increasing after shut-in, exhibiting relatively shallow spatial gradients (Figure 7). Therefore, many neighbouring patches are on a similar level of stress criticality thus increasing the likelihood for the occurrence of slip avalanches (i.e. large magnitude events), where only a small amount of stress-diffusion is sufficient to cause overcritical conditions over a larger area.

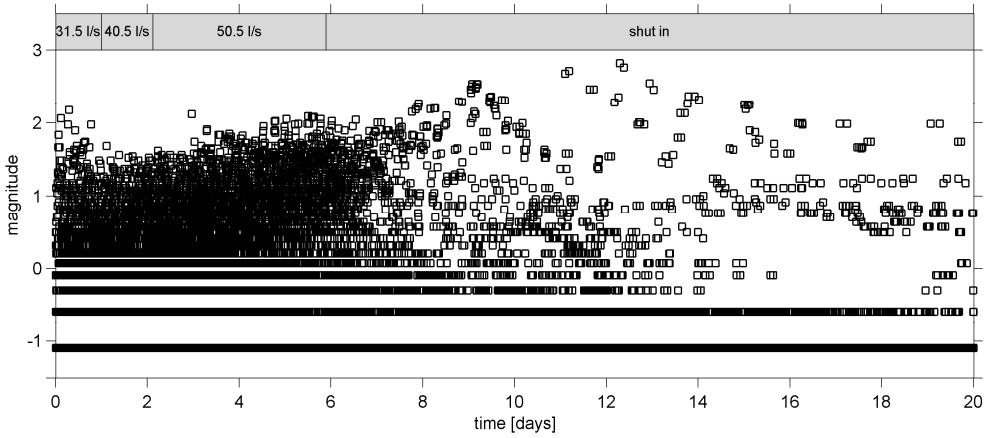

Figure 5: Magnitude of the modelled seismicity as a function of time. Top bar indicates the injection history. Note that the largest magnitude events occurred post-injection. Figure from Baisch et al. (2009b).

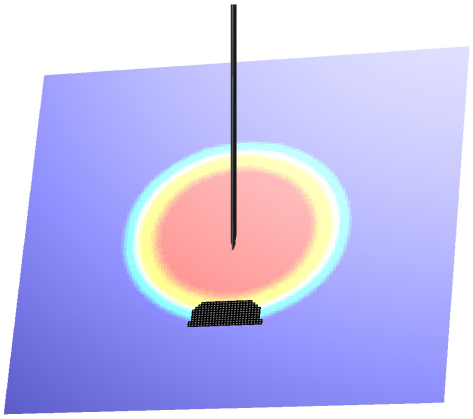

Figure 6: Distribution of hydraulic overpressures inside the fault zone at the time when the largest magnitude event occurred (after shut-in). Warm colours indicate higher overpressures. Solid line denotes the location of the injection well. Patches that slipped in the course of the largest magnitude event are marked in black.

These observations suggest that the maximum event magnitude is predominantly controlled by the area over which fluid pressure elevation brings stress conditions close to criticality. Due to this geometrical effect, the maximum magnitude of events occurring during a stimulation experiment tends to increase with injection time. In parallel, the location of seismic activity systematically migrates away from the injection well when the injection pressure remains constant.

This is the Kaiser effect typically observed in geothermal reservoirs (see section 2), which becomes most evident in Figure 8 showing radial distance from the injection well as a function of time for the modelled seismicity. The region near the injection well starts getting seismically quiet with increasing time and near-well seismicity occurs predominantly when the injection rate (and thus the injection pressure) is increased. A small number of near-well events occurring through the entire injection period reflect the slow pressure increase observed during constant rate injection. At the time of shut-in, near-well seismicity immediately vanishes (Figure 8) because fluid overpressures in the near-well region start decreasing.

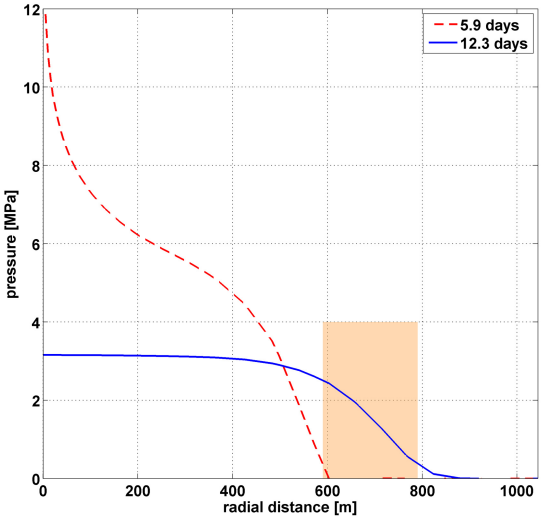

Figure 7: Modelled hydraulic overpressures inside the fault zone as a function of radial distance to the injection well for the time of shut-in (dashed line) and for the time when the largest magnitude event occurred (solid line). The shaded area marks the location of those patches slipping in the course of the largest magnitude event. At these locations, fluid overpressure increased after shut-in. Figure after Baisch et al. (2009b).

Modelled and observed seismicity exhibit similar characteristics with respect to the total number of events and the event magnitude distribution, respectively. This is demonstrated in Figure 9 which compares the two magnitude-frequency distributions. The slope of the two distributions is similar, although modelled magnitudes systematically exceed observed values by approximately 0.4 magnitude units which might be attributed to different magnitude definitions.

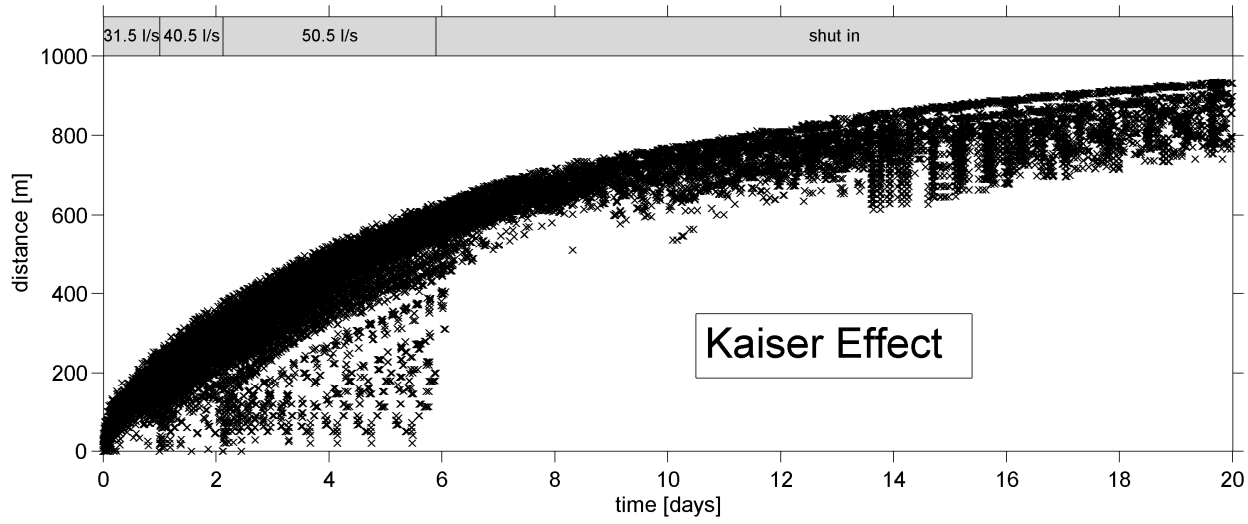

Figure 8: Radial distance of seismic events to the injection well plotted against time. Top bar indicates the injection history.

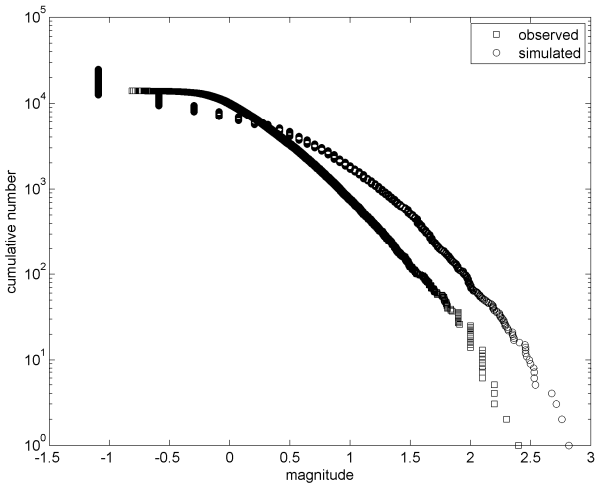

Figure 9: Magnitude frequency distribution of seismic events observed during the stimulation of the well GPK2 (squares) and modelled seismicity (circles). Figure after Baisch et al. (2009b).

5. CONCLUSIONS

Based on observations at the geothermal sites at Soultz-sous-Forêts, in the Cooper Basin, and at Basel we have discussed typical characteristics of the induced seismicity. We demonstrated that the spatial distribution of the induced seismicity is primarily controlled by two-dimensional structures most likely reflecting pre-existing (large scale) faults. A pronounced manifestation of the Kaiser Effect is observed at all three sites.

We developed a numerical model to simulate hydraulic overpressures and induced seismicity occurring inside a fault. The model is based on fluid pressure and stress diffusion with triggering of the induced seismicity being controlled by Coulomb friction. Modelled seismicity exhibits similar characteristics as observed seismicity in terms of the total number of events, the magnitude-frequency distribution, and the spatio-temporal distribution of hypocenters including the Kaiser Effect.

An intriguing observation made at different geothermal sites is that the largest magnitude events occur in the post-injection period. This phenomenon occurs also in the numerical simulations. We demonstrate that the large magnitude, post-injection events can be attributed to a simple geometrical effect without invoking other triggering mechanisms than pressure- and stress diffusion.

The numerical model presented here provides a powerful tool for addressing the seismic risk associated with reservoir stimulations and long-term circulation. For the first time, an earthquake simulator exists that can be used to model the impact of different reservoir engineering strategies on seismic activity.

REFERENCES

Baisch, S., and H.-P.Harjes: A model for fluid injection induced seismicity at the KTB. Geophys. Jour. Int., 152, 160-170, (2003).

Baisch, S., Weidler, R., Vörös, R., Wyborn, D., and L. DeGraaf: Induced seismicity during the stimulation of a geothermal HFR reservoir in the Cooper Basin (Australia). Bull. Seism. Soc. Amer., 96 (6), 2242-2256, (2006).

Baisch, S., Weidler, R., Vörös, R., and R. Jung: A conceptual model for post-injection seismicity at Soultz-sous- Forêts. Geothermal Resources Council, Trans., Vol. 30, 601-606, (2006b).

Baisch, S., Vörös, R., Weidler, R., and D., Wyborn: Investigation of Fault Mechanisms during Geothermal Reservoir Stimulation Experiments in the Cooper Basin (Australia). Bull. Seism. Soc. Amer., 99 (1), 148-158, (2009).

Baisch, S., Vörös, R., Rothert, E., Stang, H., Tischner, T., and R. Schellschmidt: A numerical model for fluid injection induced seismicity at Soultz-sous-Forêts. Submitted to Int. Jour. Rock Mech. Min. Sci, (2009b).

Bak, P., and C. Tang: Earthquakes as a self-organized critical phenomenon. J. Geophys. Res., 94(B11), 15635-15637, (1989).

Bommer, J. J., Oates, S., Cepeda, J. M., Lindholm, C., Bird, J., Torres, R., Marroquin, G., and J. Rivas: Control of hazard due to seismicity induced by a hot fractured rock geothermal project. Eng. Geol., 83, 287-306, (2006).

Charlety, J., Cuenot, N., Dorbath, L., Dorbath, C., Haessler, H., and M. Frogneux: Large earthquakes during hydraulic stimulations at the geothermal site of Soultz-sous-Forêts. Int. Jour. Rock Mech. Min. Sci.,44 (8), 1091-1105, (2007).

Cornet, F., Berard, Th., and S. Bourouis: How close to failure is a granite rock mass at a 5 km depth? Int. Jour. Rock Mech. & Min. Sci, 44, 47-66, (2007).

Davis, S. D., & C. Frohlich: Did (or will) fluid injection cause earthquakes? – Criteria for a rational assessment. Seism. Res. Lett., 64, 207-224, (1993).

Dorbath, L., Cuenot, N., Genter, A., and M. Frogneux: Seismic response of the fractured and faulted granite of Soultz-sous-Forêts (France) to 5 km deep massive water injections. Geophys. J. Int., 177 (2), 653-675, (2009).

Häring, M. O., Schanz, U., Ladner, F., and B. C. Dyer: Characterisation of the Basel 1 enhanced geothermal system. Geothermics, 37, 5, 469-495, (2008).

Hsieh, P. A., and J. D. Bredehoeft: A reservoir analysis of the Denver earthquakes: A case of induced seismicity. Jour. Geophys. Res., 86, 903-920, (1981).

Michelet, S., and M. N. Toksöz: Fracture mapping in the Soultz-sous-Forêts geothermal field using microearthquake locations. J. Geophys. Res., 112, B07315, doi:10.1029/2006JB004442, (2007).